Comparative study of API 5L X60 and ASTM 572 Gr50 Steel Exposed to Crude Oil and Seawater.

Marcy Viviana Chiquillo Márquez*, Magda Rosangela Santos Vieira, Severino Leopoldino Urtiga Filho.

* Department of Mechanical Engineering - Geosciences Technology Center - University Federal of Pernambuco. Av. Prof. Morais Rego, 1235 – University City, Recife - PE, 50670-901, e-mail address: marcy.chiquillo@ufpe.br

Abstract

In the petroleum industry, the biphasic conditions in storage and separation tanks allow that the material to remain exposed to two different environments, causing its deterioration. In this article, an evaluation is made of the corrosive behavior and Vickers microhardness (HV) of two high strength low alloy (HSLA) steels and how their surfaces are characterized. The ASTM 572 Gr50 steel showed a lower corrosion rate in all systems after being immersed for 720 and 1440 hours. Characterizing the surface by means of Scanning Electron Microscopy (SEM) showed uniform and localized corrosion for the both steels, and revealed that the ASTM 572 Gr50 steel shows pitting corrosion in crude oil systems. The electrochemical results revealed that the corrosion potential of API X60 steel was more negative; however the ASTM 572 Gr50 steel had a higher current density and a lower polarization resistance when immersed in an oil/seawater mixture. It also observed that, after being immersed in the corrosive fluids, the microstructures of the steels were not modified and variations in their microhardness (HV) were minute.

Key-words: HSLA, corrosion, crude oil, seawater, microhardness.

1. Introduction.

The need for excellent mechanical properties such as high resistance, good tenacity and weldability enhances the importance of alloy steel materials, which is why they are extensively used in the automotive industry, and for mining equipment, marine structures, sheet piling, and in daily life [1, 2]. It is a well-known fact that many uses are found for steel which contains small amounts of alloy elements such as Cr, Cu, Ni, Si and P. Such steel alloys develop good resistance to atmospheric corrosion, due to the growth of an adherent layer on the surface of materials [3-5]. In earlier studies, Y. S. Choi et al., [5] observed that elements such as Cr and Cu can produce high or low protective rust layers in aqueous environments also, just as happens when there is atmospheric corrosion. Later, Yanlei Zhou et al., observed that small amounts of elements like Cr, Mo Ni and V can enhance resistance to corrosion [3, 6]. API 5L X60 and ASTM 572 Gr50 steels are considered HSLA steels, and are widely used to manufacture stirrers, offshore platforms, pipelines and storage tanks [1, 7, 8]. The main advantage is their low cost, as compared with other steels; nevertheless, they need to withstand aggressive environments. Hence they must manifest high resistance to them. In the petroleum industry, seawater is used to recover fluid from wells. Two phases and one interfacial phase occur when seawater comes into contact with petroleum. The multiphasic corrosion created in the

mixture can be considered as one of the major problems for the metallic materials involved in this process. The zone of interface can promote a synergic effect between the oil-seawater phases, which can in turn increase bio-corrosion and corrosion when extracting and recovering petroleum and sea-water from wells, and when separating and storing petroleum [9-11].

Due to the intensive use of HSLA steels to transport and store fluids, serious problems are faced such as corrosion and the high costs of maintaining and replacing these steels [12]. This study sets out to make a comparative study between two HSLA steels with different chemical compositions, namely, API 5L X60, used in pipelines that transport petroleum, and ASTM 572 Gr50 structural steel, which is used in offshore platforms. Both are evaluated by examining the evolution of corrosion behavior, microhardness and their microstructure after these steels were exposed to seawater, crude oil and an oil/seawater mixture for a period of 1440 hours.

2. Experimental

2.1. Test specimens

Test specimens made of 40x15x5 mm coupons of API 5L X60 pipeline steel and ASTM 572 Gr 50 steel were fabricated. Their chemical composition is shown in Table 1. The surfaces of the samples were abrasively sandblasted with glass microsphere, followed by cleaning them using ultrasound equipment first with isopropyl alcohol and then with acetone for 5 seconds. Finally the specimens were left to dry [10, 13].

Table 1. Chemical compositions of the API 5L X60 and ASTM 572 Gr50 steels.

Steel	C	Mn	Si	Ni	Cu	Mo	Cr	W	V	Sn	P	S	Al	Nb	Ti
A572 Gr50	0.09	1.13	0.23	0.12	0.21	0.04	0.07	0.005	0.025	0.007	0.006	0.010	0.007	0.003	0.002
API 5L X60	0.21	0.46	0.32	0.005	0.02	0.01	-	-	-	-	0.46	0.022	0.02	0.001	0.024

2.2. Simulated Static Corrosion Tests

Simulated corrosion tests were carried out using fluid statics for 720 and 1440 hours. The specimens were exposed to three different fluids: seawater, crude oil and a mixture of crude oil/seawater. Table 2 shows the fluids used in the study. The weight loss was analysed using an analytic balance. The weight of the steels was measured before and after exposing them to the corrosive environments. After immersion, the samples underwent a procedure for cleaning after testing based on ASTM G1-03 (Standard Practice for Preparing, Cleaning, and Evaluating Corrosion Test Specimens). Hydrochloric acid was used as an etching acid (26 v/v %) and neutralization was accomplished by using sodium hydroxide (10% w/v %).

Table 2. Conditions of the fluids investigated.

Immersion systems API 5L X60 steel	Immersion systems ASTM 572 Gr50 steel	Fluids
SA	**SD**	Seawater
SB	**SE**	Crude Oil
SC	**SF**	Seawater + Crude oil (50% v/v)

2.3. Microstructure

After being immersed for 720 and 1440 hours, the samples were cut in cross section and the unexposed faces were sealed with thermoset resin. The working surface was subsequently sanded with 320, 400, 600 and 1200 grit emery papers and polished with 0.3 μm diamond paste in the polisher at 250 rpm as set out in ASTM E3-01 (Standard Guide for Preparation of Metallographic Specimens). The microstructural analysis was conducted with an Olympus Bx51M Optical Microscope, from which images with magnification to 200X were obtained.

2.4. Characterizing Microhardness and Surfaces

Microhardness tests were conducted using a microdurometer - INSIZE Auto-Turret Digital Hardness Tester Model ISH-TDV1000-B. The samples were measured after they had been cleaned and their microstructure had been analyzed (see Sections 2.2 and 2.3 above). A 1 Kgf load was used for the tests for 20 seconds of indentation. The surfaces were characterized by a TM3000 HITACHI TM3000 scanning electron microscope (SEM), to 500X magnification.

2.5. Electrochemical Experiments

2.5.1. Material Test

Electrochemical tests were performed on the square samples of API 5L X60 and ASTM 572 Gr50 steels. The coupons were soldered to copper wires using tin welding before embedding them individually in epoxy resins and leaving an exposed surface area of 100mm^2 as shown in Figure 1. Before initiating the electrochemical measurements, the surfaces of the specimens were polished using 180, 320, 400, 600 and 1200 sandpaper and polishing with a 0.3μm diamond paste. Then they were cleaned with water and ethanol, and finally blow-dried in air.

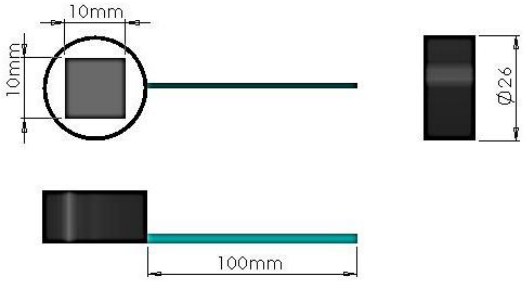

Fig 1. Coupons for electrochemical test.

2.5.2. Electrochemical Test

Electrochemical measurements were made on a three-electrode cell, with coupons (Fig. 1) as working electrodes (WE), Ag/AgCl (in saturated KCL) as the reference electrode (RE) and Platinum as a counter electrode in stagnant conditions. An Autolab Potensiostat PGSTAT 302N, operated by Nova 1.11 electrochemistry software, was used to perform the experiments. The open circuit potential (OCP) of the API 5L X60 steel versus that for ASTM 572 Gr50 steel was measured for 24 h. The linear polarization resistance (LPR) was measured by polarizing the specimens from -0.400 V to 0.400 V versus Ag/AgCl with a scanning rate of 0.5 mV/s.

3. Results and Discussions

3.1. Corrosion Rate

Figures 2a and 2b show the evolution of the weight loss and corrosion rate of both steels after 720 and 1440 hours of exposure to fluids. Figs 2a and 2b show that the corrosivity of the seawater is higher than that for the crude oil systems. Note that the SA and SD systems have a greater weight loss and higher corrosion rate when compared to those of the other systems. Wemming et al., and Miao et al., show that the presence of Cl^- increases corrosion, thereby generating a greater weight loss in seawater systems. It is a well-known fact that the process of electrochemical corrosion results from the orderly flow of electrons. Hence, in the SB and SE systems, the phenomenon of corrosion is less because the crude oil is highly resistive, thus avoiding any flux and reducing the process of corrosion [7, 14, 15]. The SC and SF systems show high weight loss and a high corrosion rate in comparison with those of the SB and SE systems but less so than those of the SA and SD systems. This is expected because the high chloride content in seawater and different compounds in the crude oil can create a synergism that is increasingly aggressive towards the environment [2, 10, 11, 16]. Figure 2a shows a great weight loss in the API X60 steel when it is exposed to all the environments, as was mentioned above. Some elements present in the ASTM 572 Gr 50 steel can generate a layer of corrosion in aqueous environments, which can avoid attacks of corrosion on the environment, thus providing some protection for this steel and causing less weight loss as compared to that for the API X60 steel.

On analyzing the corrosion rate (Fig 2b), we observed a decrease of the values for the systems when the exposure time increases; when the samples are exposed continually to the corrosive environment, they began to corrode and biofilm grew on the surface of the material. This biofilm acts as a physical barrier, thereby hindering contact with the fluid and surface of the material and thus reduces the reaction rate. The samples of API X60 steel in the SA system do not display the same behaviour. In this case, the corrosion rate increases in the interval of immersion between 720 hours to 1440 hours. This was attributed to the rust layer formed during the immersion process not being sufficiently stable and so it became detached, which led to electrochemical corrosion and hence, the corrosion rate increased. According to the NACE-RP-07-75 (Standard Practice Recommended Preparation, Installation, Analysis and Interpretation Corrosion Coupons in Oilfield Operations), the values of the

corrosion rate of both steels are classified as being moderate, except the samples immersed in SB and SE systems which are classified as having low corrosion.

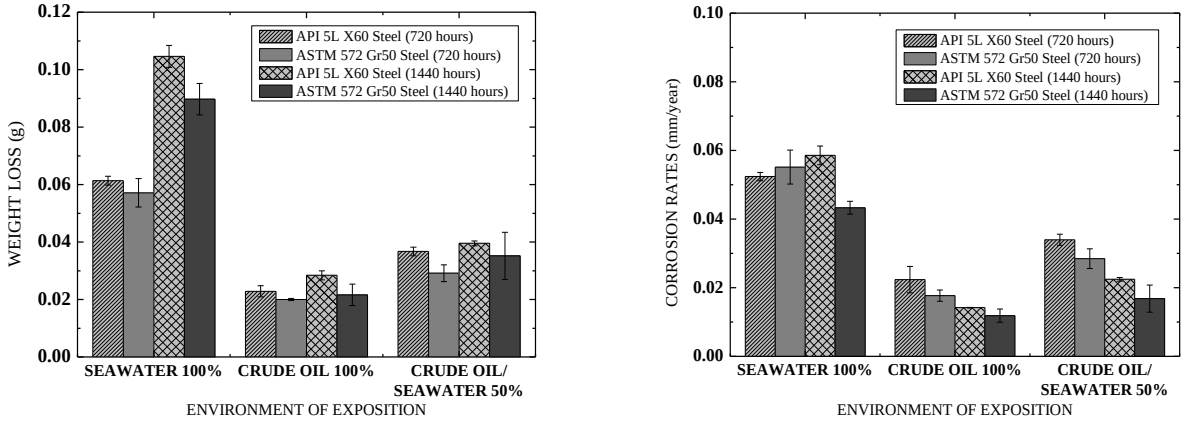

a] b]

Fig 2. Results of API 5L X60 and ASTM 572 Gr50 steels. [a] Weight loss [b] Corrosion rate.

4. Analysis of the Microstructure and Surface

The main importance of the systems investigated in this study lies in the fact that they are of great use in the petroleum industry. The conditions of simulated storage tanks were studied as two phases of the fluids and an interface region formed. Fig. 3 shows the surface of the samples after sandblasting, without immersing them in any corrosive fluid. These were considered as a benchmark for comparison with the results after immersion. Figure 4 shows the morphologies of the surface samples after the corrosion product layer had been removed. The surfaces of both the steels, after being immersed for 1440 hours, seem to be more severely attacked when compared with the samples that were immersed for 720 hours. By comparing Figure 3 and Figure 4 we can observe changes in the surfaces of all systems with the presence of uniform and localized corrosion. However, it is worth noting that although the corrosion rate is moderate or low as discussed in Section 3.1, more care needs to be taken when localized corrosion is present in order to avoid future accidents. It is evident in all the systems that the presence of localized corrosion highlights the aggressiveness in the fluids of the petroleum industry (seawater and crude oil). The presence of high amounts of chlorides in seawater justifies the localized corrosion, but it is also interesting that this mechanism was identified in the samples exposed to crude oil [1, 17, 18]. The existence and performance of microorganisms in metabolite acids can account for why this kind of corrosion arises and why localized attacks (pitting, shallow cavities, alveolar corrosion) occur [16, 19, 20, 21]. As Figs. 4a and 4e show, the API X60 steel immersed in the SA system presents alveolar corrosion with small cavities which have a maximum length of 108.0 μm. On the other hand, the ASTM 572 Gr50 steel immersed in the SD system has cavities with a maximum length of 86.17μm, thus emphasizing most attacks on API 5L X60 steel exposed to this system have seawater only.

The systems containing crude oil only (SB and SE) showed localized attacks taking place through small holes with a diameter of 57.45μm in the API X60 5L steel. In the same way, holes with a

diameter of 40.43 μm, can be observed in the ASTM 572 Gr 50 steel, some of which are considered as pitting corrosion as their surface diameters are greater than their depth. From Figs. 4c, d, g and h, note that the presence of two different fluids in SC and SF systems generates uniform corrosion and localized corrosion for both steels, thus highlighting that the zone exposed to the seawater has cavities of greater length and more holes than the zone exposed to the crude oil for the same sample. In accordance with Section 3.1, the API X60 steel shows a higher corrosion rate than that of the ASTM 572 steel in all the fluids to which it was exposed and these micrographics (Fig 4) enabled it to be corroborated that most attacks were on the surface of this steel.

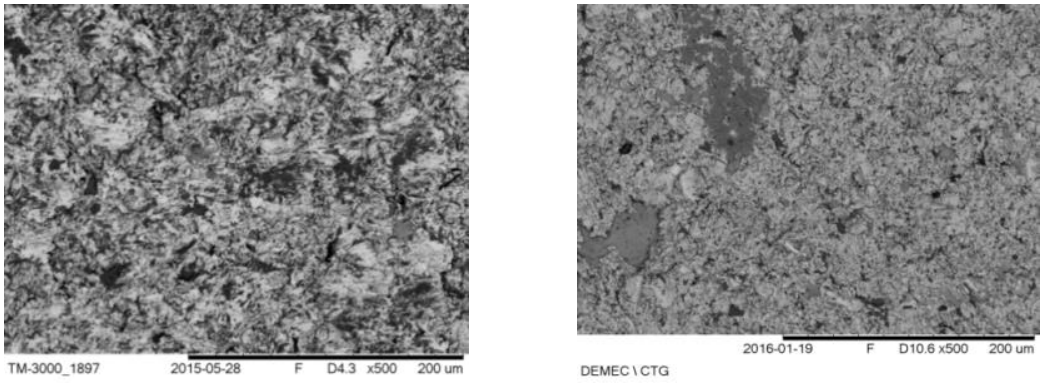

a] **b]**

Fig 3. SEM of surfaces samples after sandblasting. [a] API 5L X60 steel, [b] ASTM 572 Gr50 steel.

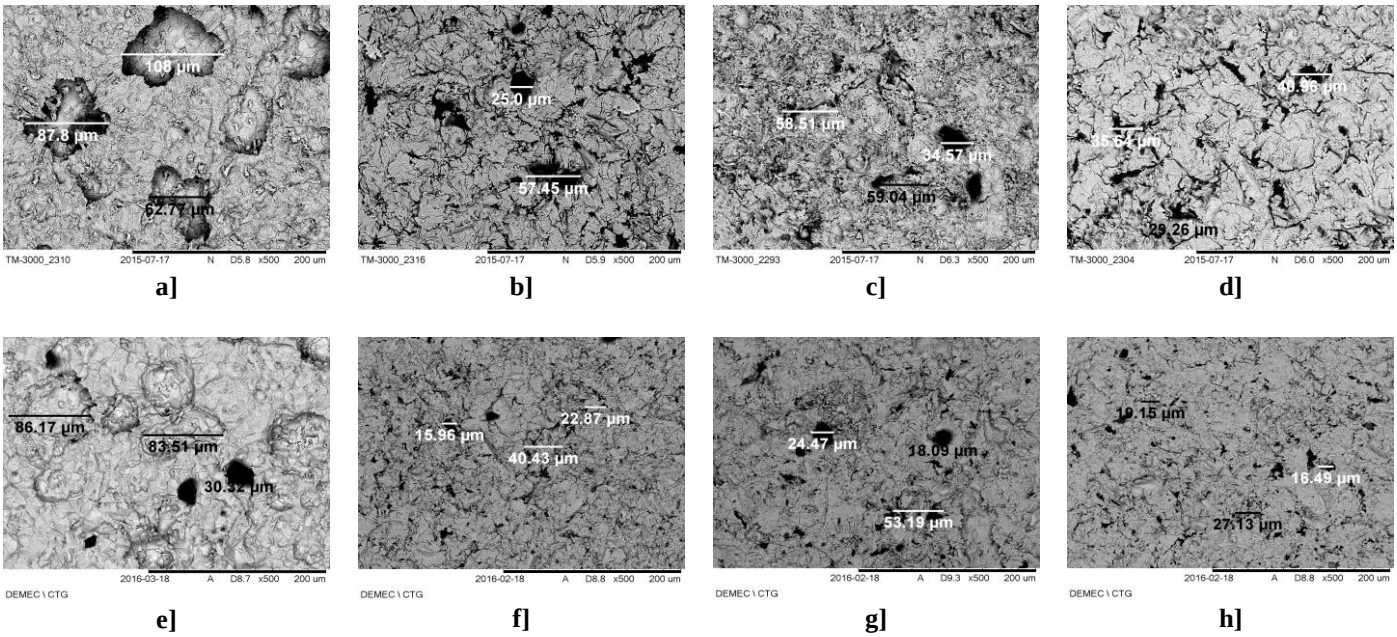

a] **b]** **c]** **d]**

e] **f]** **g]** **h]**

Fig 4. SEM of surfaces samples after 1440 hours of exposure. [a] SA System, [b] SB System, [c] SC System (Seawater), [d] SC System (crude oil), [e] SD System, [f] SE System, [g] SF System (Seawater), [h] SF System (crude oil).

Figure 5 shows the microstructural results for the surface section of the API 5L X60 steel and the ASTM 572 Gr50 steel before they were exposed to corrosive environments. Our findings show the typical ferrite-pearlite microstructure of HSLA steels; here the microstructure has darker pearlite regions and lighter ferrite regions [22-24]. As described in Table 3, following the ASTM E112-13 Standard (Test Methods for Determining Average Grain Size), note that there is a greater amount of pearlite in the API 5L X60 steel than in the ASTM 572 Gr50 steel. This is expected because of the amount of carbon in its composition. The alloyed elements such as V, Ti, Nb present in the ASTM 572 Gr 50 steel make the grain more refined than that of the API 5L X60 steel. Note also that the size of the grain and the different types of constituents are some of the principal factors which can influence mechanical properties such as the strength, the ductility and the toughness of steels [6, 24, 25, 26]. Fig. 6 shows the microstructure of the steels after 1440 hours of exposure in seawater. From Fig. 6a we identified that the microstructure of API 5L X60 steel is formed by alternate bands of pro-eutectoid ferrite and pearlite in a matrix predominantly of ferrite; magnification of the micrograph shows that the pearlite is completely resolved with alternate lamellae of ferrite and cementite (Fig 6b).

Table 3. Quantification of the phase and grain size of the surface section.

Steel	**Compound**	**Amount phase (%)**	**Average size** (μm)
API 5L X60	Pearlite	11.308	29.468
	Ferrite	88.692	
ASTM 572 Gr50	Pearlite	9.488	18.847
	Ferrite	90.512	

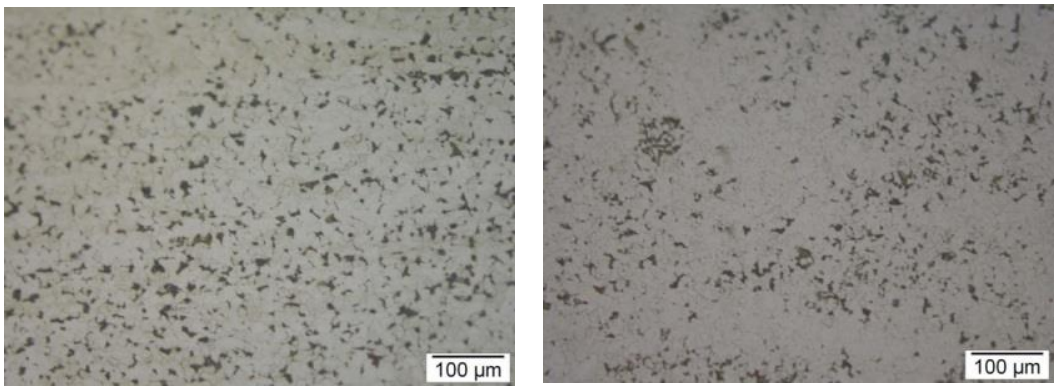

a] **b]**

Fig 5. Microstructure of steels after sandblasting. [a] API 5L X60, [b] ASTM 572 Gr50

The microstructure of ASTM 572 Gr50 is composed of a ferritic matrix and degenerated pearlite colonies with a lesser amount of cementite (dark) which is generated from the amount of carbon in it and the hot treatment received (Fig 6 c and Fig 6 d). After 1440 hours of exposure, none of the corrosive environments caused significant changes to the microstructures of the steel (intergranular corrosion, grain size, change of phases).

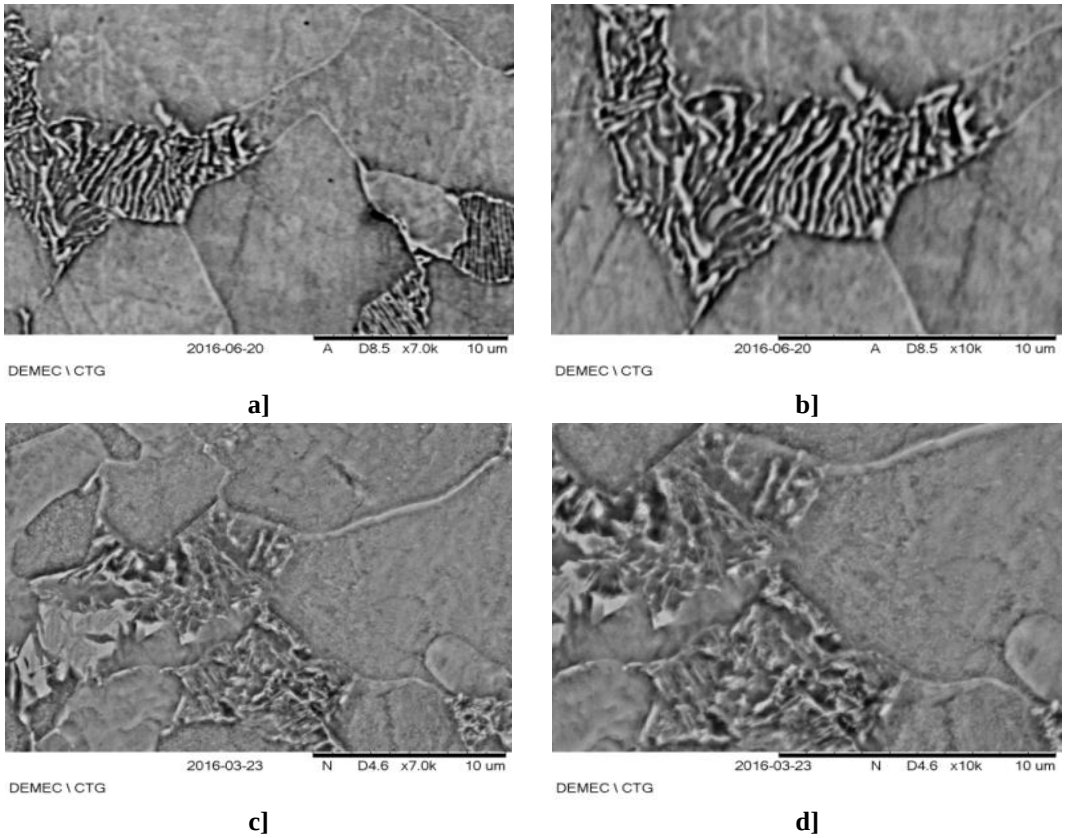

Fig. 6 Microstructure results after 1440 hours of immersion. [a-b] API 5L X60, [c-d] ASTM 572 Gr50.

5. Microhardness

Figure 7a and Figure 7b show the results of the Vickers microhardness (HV) test for the API 5L X60 and ASTM 572 Gr50 steels after removal of the rust layer and metallographic preparation – see Sections 2.1 and 2.2. It should be noted that the measurements of HV for the samples of SC and SF systems were made in the zones exposed to crude oil as well as in those exposed to seawater.

To evaluate the behavior of the microhardness values throughout the process, we took a benchmark which gave values of 148 and 168 (HV1) for X60 and ASTM 572 respectively. Figure 7a shows values where the ASTM 572 steel has greater microhardness; a high amount of elements such as Cu, Cr, Mo Si and Mn present in the steel which slightly increased the strength of the ferrite, and also increased resistance to the penetration of steel. In addition, the elements Ti, Nb and V help to refine the grain, which is an effective strengthening mechanism to improve mechanical properties [3, 6, 24, 27, 28, 29]. After immersion and following Section 2.2 for metallographic preparation, note that the samples show slight changes in their values as compared to the reference patterns which are normal due to the non-homogenous microstructure (Fig. 5). The sample pattern after sandblasting has values of 205 and 224 (HV1) for API X60 and ASTM 572 steels, respectively. In Figure 7b, note that these values change slightly after the exposure time; the SA, SB and SC systems have values in the range of 196 to 211 (HV1) while the SD, SE and SF have values in the range of 199 to 227; the change

perceived can be attributed to the corrosion suffered by the surface of the samples; ASTM 572 shows values above those for API X60 in proportion to the alloy elements present. According to Gonzales and Machado, the sandblasting process can produce a change in the microstructure of steel near its surface, thereby generating a change in its microhardness values [30]. On analysing Figure 7a and Figure 7b, note that after sandblasting the microhardness values of the surface in the samples are higher than those obtained after metallographic preparation. This been attributed to the pressure exerted during sandblasting, and after polishing the affected zone is removed showing lower values are found as compared to those from immersion (after sandblasting).

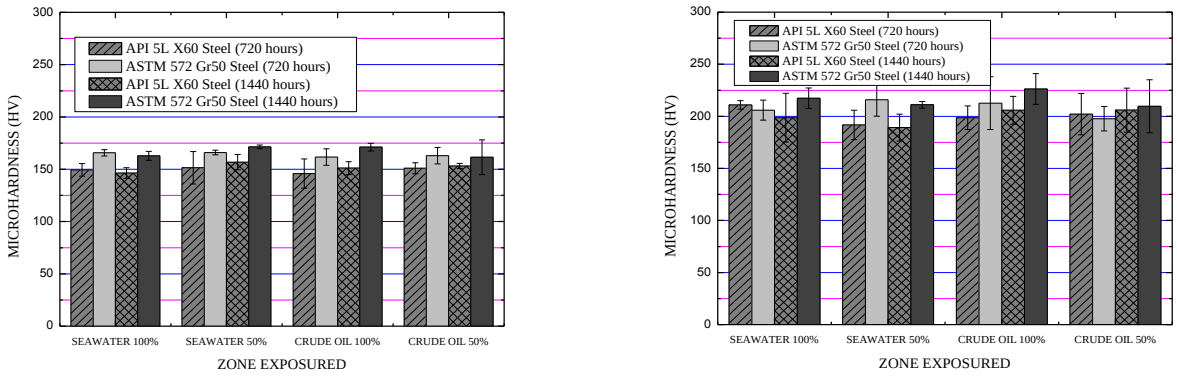

a] b]

Fig 7. Vickers microhardness results, after 720 hours and 1440 hours of immersion
[a] metallographic preparation, [b] the removal of the layer rust.

6. Electrochemical Test

6.1. Measurements of Open Circuit Potential (OCP)

Electrochemical measurements of Open Circuit Potential (OCP) were made and Potentiodynamic polarization curves were plotted so as to determine E_{corr} and I_{corr}. Fig. 8 illustrates the evolution of OCP over time for the API X60 and ASTM 572 steel after 24 hours of immersion both in seawater (SA, SD systems) and in a mixture of seawater and crude oil (SC, SF systems). The OCP curves show that at the initial test time a more negative potential value was obtained for the electrolyte from the SC system (-0.621 V/Ag/AgCl); after one hour of exposure, the analyses showed that the potential of the steels increased towards the more negative values from the first moment that the electrode was immersed. This was a result of an oxide film, which had formed on the work electrode surface, dissolving [1, 18, 31, 32].

The open circuit in the first 5h of exposure to the SA and SC systems of the API X60 steel has similar corrosion potential. These results show that the fluid stagnation in the mixture promotes little change in the aggressiveness of these fluids. In addition, from these time values, the behaviour of the potential is relatively stable which is due to the formation of the oxide layer that provided a partial protection for the steel, thus avoiding complete dissolution [1, 18, 31, 33]. For the two systems of ASTM 572 steel, after 8 hours of exposure to the fluids, the following values of constant potential were observed,

-0.674 V (Ag/AgCl) and -0.682 V (Ag/AgCl) SD and SF respectively, which makes a small difference between their corrosion potentials. The OCP results indicate that the surface of the API X60 steel is less corrosion resistant than that of ASTM 572 steel over the same conditions; for longer times of exposure (24h), the behaviour of the materials is practically the same in both fluid conditions (seawater and oil/seawater), this being attributed to corrosion deposits forming on their surfaces.

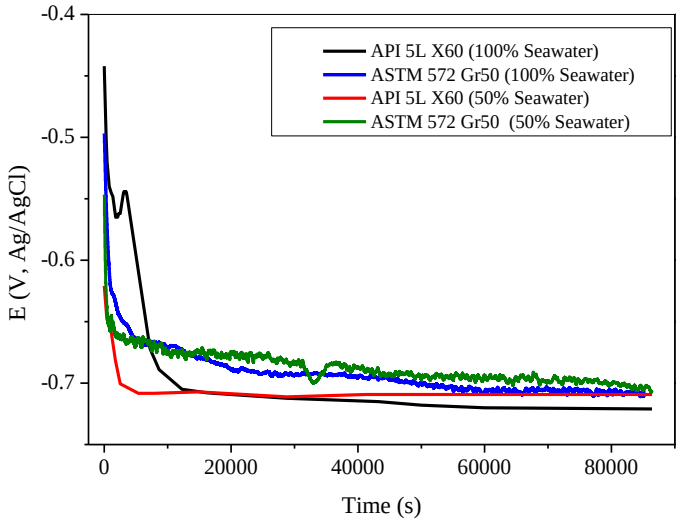

Fig 8. The OCP measurements for API X60 and ASTM 572 steels.

6.2. Potentiodynamic Polarization Measurements

Figure. 9 depicts the results of Potentiodynamic polarization for both the steels when placed in aerated, stagnant conditions, in seawater and in seawater/crude oil fluids. The values of β_c (cathodic) and β_a (anodic) Tafel Slope, the corrosion current density (J_{corr}), polarization resistance (R_p) and corrosion rate (CR) obtained from polarization curves are listed in Table 4. The corrosion rate was calculated, as set out in ASTM G102 (Standard Practice for Calculation of Corrosion Rates and Related Information from Electrochemical Measurements), by using Equations 1, 2 and 3:

$$J_{corr} = \frac{B}{Rp} \quad (1)$$

Where,

$$B = \frac{(\beta_a \beta_c)}{2.3(\beta_a + \beta_c)} \quad (2)$$

Therefore, the corrosion rate (CR) is calculated as:

$$CR = \frac{J_{corr} KW}{\rho A} \quad (3)$$

Where:

K is a constant that defines the units for CR (3272 mm/(amp.cm.year));
W is the equivalent grams of steel (27.93gram/equivalent);
ρ is the density of Fe (7.86 g/cm^2);
A is the area of the exposed surface of the electrode work in cm^2;

It has been reported by several authors that the anodic reactions that occur in steels due to their being exposed to solutions containing chlorides can be described by Equations (5) and (6). The cathodic reactions in steels with or without the presence of oil can be explained by Equation (7) [1, 7, 17, 34-36].

$$Fe^{2+} \rightarrow Fe + 2e^{-} \quad (5)$$

$$Fe^{3+} \rightarrow Fe + 3e^{-} \quad (6)$$

$$O_2 + 2H_2O + 4e^{-} = 4OH^{-} \quad (7)$$

When the surface develops a partially protective oxide layer, which can happen with different possible oxides, this can be described by Equations (8) and (9)

$$Fe + \frac{1}{2}O_2 + H_2O \rightarrow Fe(OH)_2 \quad (8)$$

$$3Fe(OH)_2 + \frac{1}{2}O_2 \rightarrow Fe_3O_4 + 3H_2O \quad (9)$$

According to Eq. (9), in the presence of aerated conditions the $Fe(OH)_2$ can generate a rust layer (Fe_3O_4) which provides partial protection to the surface of the steel, thereby limiting spontaneous degradation. It is worth noting that the rust layer can be dissolved when the potential applied is (positively) increased. Fig. 9 shows the Tafel curves. In general, all the samples exhibit an active behaviour in both electrolyte conditions; Fig. 9 shows that the API X60 steel, in the presence of oil (SF systems), has more positive values of corrosion potential and a higher cathodic current than those of the samples in seawater conditions. This is due the fact that an oily film is formed on the surface that acts as a partial protection for the steel. In addition, the dissolution of oxygen is more favourable in the oil/seawater emulsion. Oil does not contain any polar molecules of hydrocarbons which have better interaction with the oxygen apolar molecules, thus making it difficult to reduce oxygen (Eq. 7).

Table. 4 Parameters obtained from potentiodynamic polarization curves for SA, SC, SD and SF systems

Sample	E_{CORR} (mV)	j_{CORR} (mV)	β_a (mV/dec)	β_b (mV/dec)	CR (mmy^{-1})
API X60 (Seawater 100%)	-705.7	4.66	82	380	0.050
API X60 (Seawater 50%)	-682.9	4.20	100	300	0.049
ASTM 572 (Seawater 100%)	-548.0	1.12	59	96	0.013
ASTM 572 (Seawater 50%)	-625.4	17.6	80	250	0.204

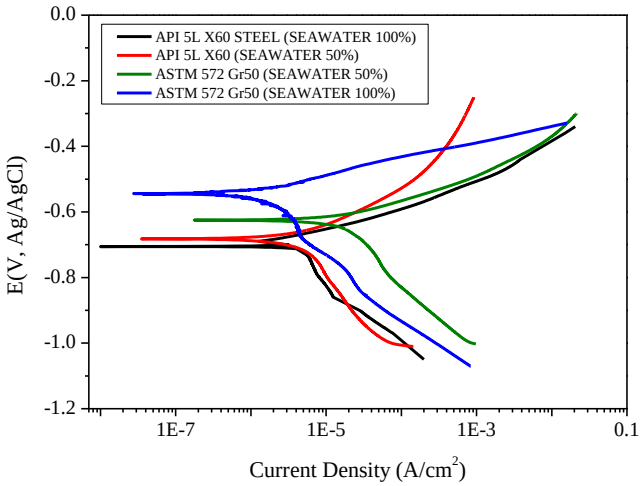

Fig 9. Potentiodinamyc polarization results for API X60 and ASTM 572 steels.

Zhang and Cheng conducted studies on potentiodynamic polarization for API X65 steel in oil/water emulsion conditions, and found a low cathodic current for the samples exposed to seawater. In our case the API X60 steel presented the same behavior as in their investigation and ASTM 572 steel showed a higher cathodic current for the sample in the seawater system. The sample submitted to electrolyte constituted by crude oil/ seawater emulsion shows the highest current density ($17.6mV$) and the highest corrosion rate values (Table 4). Such behavior may be associated with the material being more susceptible to corrosion pitting which is generated because this fluid is so aggressive, as shown in Fig. 4 (SC and SF systems). The samples exposed to these systems showed corrosion pitting, in addition, to the dissolution of corrosive compounds from the oil phase, mainly to the sulphides typically derived from crude oil. This could cause this electrolyte to be more aggressive for these steels [10, 21, 36].

The potentiodynamic polarization curves evidence the increase of the anodic current density corresponding to the increase in the potential values for both steels, where the SD system (crude oil/seawater mixture) has a higher E_{corr} compared with that of the SF system. It can corroborated that API X60 steel is more susceptible to the corrosion process than ASTM 572 steel which is less affected; despite the presence of the pearlite, the micro-constituent is more stable. It is worth mentioning that Fig. 5 shows that it is the microstructure of API X60 steel which has the greatest amount of pearlite along with ferrite present. This allows many more micro-chemical cells to be created resulting in more active sites that enhance corrosion.

By comparing the electrochemical results of SA and SD systems with the results obtained by gravimetric tests for the samples exposed to seawater, the corrosion rate for the 60 days of exposure shows that the values so obtained are different for the two methods. In the gravimetric test, the sample will be subjected to continuous changes in the surface of the material during the exposure time, thus generating more weight loss, and therefore the corrosion rate is modified (Fig. 2). While in linear polarization, an accelerated result is obtained from the test, this would not be exactly the actual exposure condition, since a potential difference is being established in the material. Another important factor worth mentioning is that this may have influenced the difference in the corrosion rate obtained for the different types of test. While in the weight loss tests, the parts were exposed to the corrosive medium after the abrasive blasting, the samples submitted to the Polarization test were submitted to the metallographic preparation procedure at the polishing stage.

Conclusions

This article examined the corrosive behavior of API 5L X60 and ASTM 572 Gr 50 steels when exposed to seawater and crude oil by means of gravimetric, electrochemical, microhardness and surface characterisation. After 1440 hours of immersion, the corrosion rate of the ASTM 572 Gr50 steel was less than that of the API 5L X60 steel in the fluids. We conclude that the samples have a higher corrosion rate when immersed in seawater systems (SA and SD). The SB and SE systems show less weight loss due to the high resistivity of crude oil, and thus avoid accelerated corrosion. But it should be noted that the samples have, nevertheless, suffered corrosion. According to NACE-RP-07-75, the corrosion rate for the steels obtained in this study is classified as moderate except the samples immersed in the SB and SE systems which are classified as having a low corrosion rate. The corrosion process has no effect on the microhardness results after and before the immersion process, thereby highlighting that the ASTM 572 Gr50 steel has a higher value of Vickers microhardness than API 5L X60. This happened due to the alloys present. Characterization of the surface shows uniform and localized corrosion for both steels where it is observed that the ASTM 572 Gr50 steel is more susceptible to a pitting attack among all the systems studied. The electrochemical behaviour of different fluids for the steels was different, which showed that the ASTM 572 Gr50 steel has more current density when exposed to oil/seawater than API X60. Thus, less polarization resistance was seen in the SF system. The ASTM 572 steel showed less current density in the seawater systems. Thus, these samples have the highest polarization resistance among all the systems, thus making this steel less susceptible to corrosion.

Acknowledgements

This work was supported by CAPES, UFPE, FINEP, CNTM and the Laboratory of Composite Materials and Structural Integrity of the Department of Mechanical Engineering, Federal University of Pernambuco.

REFERENCES

[1] E. M. Sherif, *Molecules*. **2014**, 9962.

[2] R. E. Melchers, R. J. Jeffrey, *Proceedings of the Institution of Civil Engineers.* **2015**, 167, 159.

[3] W. Liu, Q. Zhou, L. Li, Z. Wu, F. Cao, Z. Gao, Journal of Alloys and Compounds. **2014**, 598, 198.

[4] Y. Zhou, J. Chen, Y. Xu, Z. Liu, *Journal of Materials Science & Technology.* **2013**, 29, 168.

[5] Y. S. Choi, Y. G. Kim, *Corrosion.* **2000**, 1202.

[6] E. C. Bain, H. W. Paxton, *Alloying Elements in Steels*, ASM, Cleveland, Ohio, USA, **1939.**

[7] G. A. Zhang, Y. F. Cheng, *Corrosion Science*. **2009**, 901.

[8] J. C. Ferreira, L. F. Guimarães, E. S. Marouco, O. Ribeiro, *Soldagem & Inspeção.* **2015**, 20, 347.

[9] F. F. Elian, E. Mahdi, Z. Farhat, A. Alfantazi, *Electrochemical Science.* **2013**, 3026.

[10] M. R. Vieira, *Ph. D. Thesis*, UFPE Recife, Brasil, **2013**.

[11] M. R. Vieira, *MSc. Thesis*, UFPE Recife, Brasil, **2008**.

[12] V. Panaite, V. Musat, F. Potecasu, C. Gheorghies, *Metalurgia*. **2011**, 63, 13.

[13] E. Dantas, Geração de vapor e água de refrigeração, Ecolab, Brasil, Rio de janeiro, **1988.**

[14] M. M. Stack, G. H. Abdulrahman, *Wear*, **2012**, 274.

[15] H. Q. Becerra, C. Rematoso, D. D. Macdonald, *Corrosion Science*. **2000**, 561.

[16] S. Belkaid, M. A. Ladjouzi, S. Hamdani, *Journal Solid State Electrochemical*, **2011**, 15, 525.

[17] R. O. Rihan, *Material Research.* **2013**, 16, 227 .

[18] A. Rauf, E. Mahdi, *International Journal of Electrochemical Science.* **2012**, 7, 5692.

[19] V. Gentil, *Corrosão.* Livros Técnicos e Científicos editora S.A, Rio de Janeiro , Brasil, **2011**.

[20] H. A. Videla, *Biocorrosão, biofouling e biodeterioração de materiais,* Edgard Blucher Ltda, São Paulo , Brasil, **2003**.

[21] N. C. Barros, MSc. Thesis, UFRJ Rio de Janeiro, Brasil, **2015**.

[22] P. R. Mei, A. L. Silva, *Aços e Ligas Especiais,* Edgard Blucher, São Paulo, **2008**.

[23] H. Colpaert, *Metalografia dos Produtos Siderúrgicos Comuns*,Blucher, São Paulo **2008**.

[24] L. B. Bramfitt, *Metals Handbook Desk Edition,* J.R. Davis, Bethlehem, **1998**.

[25] R. Kuziak, T. Bold, Yi-Wen Cheng, *Journal of Materials Processing Technology*, **1995**, 53, 255.

[26] R. L. Miller, *Metallurgical Transactions.* **1972**, 3, 905.

[27] *K*. Muszka, J. Majta, L. Bieinias, *Metallurgy and Foundry Engineering.* 2006, 32, 87.

[28] D. Clover, B. Kinsella, B. Pejcic, R. de Marco, *Journal of Applied Electrochemistry.* **2005**, 35, 139.

[29] *L*. Zhang, A. Ma, J. Jiang, X. Jie, *Materials and Desing.* **2015**, 65, 115.

[30] M. A. Calle, I. F. Machado, Presented at the congress ABCM, Uberlandia, Brasil, 18 May - 21 May, **2003**. pp. 1-10.

[31] E. M. Sherif, A. A. Almajid, K. A. Khalil, H. Junaedi, F. H. Latief. *International Journal of Electrochemical Science.* **2013**, 8, 9360.

[32] W. Liu, H. Zhang, Z. Qu, Y. Zhang, J. Li, *Journal Solid State Electrochemical.* **2010**, 14, 965.

[33] S. Choudhary, A. Garg, K. Mondal, *Journal of Materials Engineering and Performance.* **2016**, 25, 2969.

[34] O. I. Sekunowo, S. O. Adeosun, G. I. Lawal, *International Journal Of Scientific & Technology Research.* **2013**, 2, 139.

[35] L. P. Nunes, *Fundamentos de Resistência à Corrosão,* Interciência Ltda, Rio do Janeiro, Brasil, **2007**.

[36] Y. Liu, B. Zhang, Y. Zhang, L. Ma, P. Yang, *Engineering Failure Analysis*. **2016**, 60, 307.